CHEMISTRY OF MATERIALS

Communication

pubs.acs.org/cm

Tuning the Pore Size of Ink-Bottle Mesopores by Atomic Layer Deposition

Jolien Dendooven,[†,*] Bart Goris,[‡] Kilian Devloo-Casier,[†] Elisabeth Levrau,[†,§] Ellen Biermans,[‡] Mikhail R. Baklanov,[∥] Karl F. Ludwig,[⊥] Pascal Van Der Voort,[§] Sara Bals,[‡] and Christophe Detavernier[†]

[†]Department of Solid State Sciences, COCOON, Ghent University, Krijgslaan 281/S1, B-9000 Ghent, Belgium

[‡]EMAT, University of Antwerp, Groenenborgerlaan 171, B-2020 Antwerp, Belgium

[§]Department of Inorganic and Physical Chemistry, COMOC, Ghent University, Krijgslaan 281/S3, B-9000 Ghent, Belgium

[∥]IMEC, Kapeldreef 75, B-3001 Leuven, Belgium

[⊥]Physics Department, Boston University, 590 Commonwealth Avenue, Boston, Massachusetts 02215, United States

Supporting Information

KEYWORDS: *ALD, electron tomography, ellipsometric porosimetry, X-ray fluorescence, mesoporous titania, porous film*

Mesoporous materials are of great interest to a broad range of applications, for instance, in optical, electronic, and sensor devices, in molecular separation, and, especially, in heterogeneous catalysis.[1,2] Ordered mesoporous oxides, such as the MCM and SBA families, are considered promising catalyst supports because of their uniform pore size and high surface area. For a long time, the focus has mainly been on materials possessing one-dimensional (1D), hexagonally ordered mesopores, such as MCM-41 and SBA-15. Over the last years, three-dimensional (3D) structured supports have gained more interest because they are expected to allow for faster transport and diffusion of the reactants and products. The so-called cage-like materials, such as SBA-16, have a 3D network of spherical cages connected to each other via smaller pore necks. Despite the numerous applications of these structures, there is an increasing demand toward flexible tuning of the pore sizes as well as functionalization of the pore walls.[3]

Atomic layer deposition (ALD) is a promising technique for tailoring mesoporous materials.[4] This thin-film growth method relies on sequential self-terminating gas−solid reactions separated by evacuation steps. Direct advantages of the self-limiting nature of the chemical reactions are the atomic level control of the deposited film thickness and the ability to uniformly coat the interior surface of porous materials. Consequently, under optimized process conditions, ALD can be used to modify both the pore size and the chemical composition of the pore walls in a controlled way. So far, this has mainly been demonstrated in materials having a 1D channel-like pore system such as anodic aluminum oxide membranes[5,6] and SBA-15[7,8] and in materials without a specific pore system such as mesoporous silica gels,[9] aerogels,[10] and ultrastable Y zeolites.[4,11] In the present study, we explore the potential of ALD for tuning the pore size of cage-like, or ink-bottle shaped, mesopores at the atomic level. This is challenging because the pores are only accessible via narrow, nanometer sized channels and most vapor deposition techniques, such as physical vapor deposition and conventional chemical vapor deposition, will therefore result in pore clogging rather than in the desired modification of the pore size.

We used ALD to deposit ultrathin TiO_2 and HfO_2 layers in a mesoporous titania film containing ink-bottle shaped pores. Both ALD processes were monitored in situ using X-ray fluorescence (XRF).[12] The final structure of the TiO_2 coated film was examined using ellipsometric porosimetry (EP),[13] whereas the HfO_2 coated one was characterized by electron tomography. This latter technique provides a direct and local characterization of the inner 3D structure of the coated mesopores. Our detailed investigation demonstrates that both ALD processes allow for atomic level tuning of the size of ink-bottle mesopores. Furthermore, it is confirmed that in situ XRF is an excellent technique to monitor ALD processes in mesoporous thin films.

Porous titania films with a thickness of 120 nm were synthesized according to a method previously published by Pan and Lee[14] as detailed in the Supporting Information. The shape and the size of the pores were determined through EP.[13] The toluene sorption isotherm measured on the original titania thin film indicated a porosity of ca. 27% and showed hysteresis due to capillary condensation of toluene in the mesopores (Figure 1a). On the basis of its shape, this hysteresis loop is categorized as an H2 type loop in the IUPAC classification, a type that is often associated with ink-bottle shaped mesopores. Shrinkage of the porous film was observed in the relative pressure range where capillary condensation of toluene in the mesopores occurred (Figure S1 in the Supporting Information).[13,15] The shrinkage effect was much more pronounced during desorption than during adsorption. As further explained in the Supporting Information, this behavior presents solid proof for the presence of ink-bottle shaped mesopores in the titania thin film. Finally, the pore size and neck size distribution are shown in Figure

Received: December 17, 2011
Revised: April 17, 2012
Published: May 3, 2012

ACS Publications © 2012 American Chemical Society

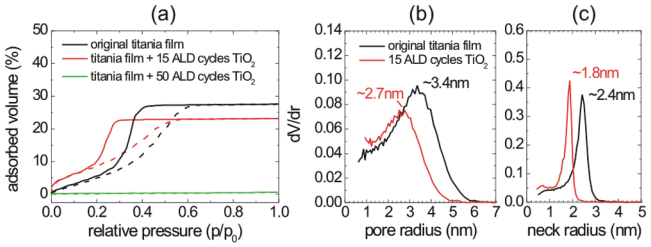

Figure 1. (a) Toluene sorption isotherms determined using EP on different pieces of the same mesoporous titania film subjected to 0, 15, and 50 TiO_2 ALD cycles. (b/c) Pore/neck size distribution evaluated from the adsorption/desorption branches in (a).

1b,c, respectively, and indicate an average pore diameter of ca. 6.8 nm and an average neck size of ca. 4.8 nm.

Figure 2a–d schematically shows how conformal deposition by ALD is expected to proceed in ink-bottle mesopores. Using

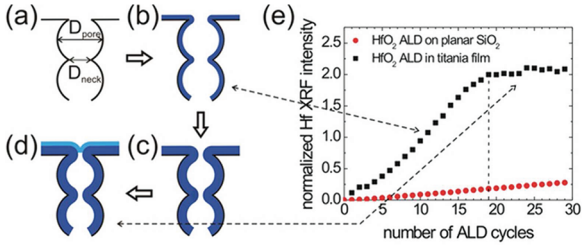

Figure 2. (a–d) Schematic representation of conformal ALD in ink-bottle mesopores. (e) In situ XRF during HfO_2 ALD on a planar SiO_2 substrate and on a mesoporous titania film: Hf Lα (7.9 keV) peak area against the number of ALD cycles.

ALD, the pore walls are uniformly coated in a layer-by-layer fashion until the size of the neck becomes too small for the precursor molecules to enter the pores (Figure 2b,c). From that point onward, ALD continues on top of the coated ink-bottle mesopore (Figure 2d). Note that the ink-bottle shape implies that the spherical cages are not completely filled but that some porosity remains upon conformal coating by ALD. Remaining porosity as a consequence of the conformal nature of ALD was earlier observed after filling of a silica opal film[16] and coating of tobacco mosaic viruses having 4 nm wide tubular channels.[17] In the straight viral mesopores the incomplete filling was explained by exclusion of the precursor molecules from the hollow channels upon reaching a critical pore size.

The mesoporous titania thin film was coated with HfO_2 using ALD, as explained in the Supporting Information. The Hf-uptake per ALD cycle was monitored in situ by the Hf Lα fluorescent signal (Figure 2e). Figure 2e also shows the result for ALD of HfO_2 on a planar SiO_2 surface. As expected for ALD on a planar substrate, the Hf XRF intensity increased linearly with the number of cycles.[18] An X-ray reflectivity measurement after 30 ALD cycles revealed a growth per cycle (GPC) of 1.2 Å on the planar substrate. During the first ca. 19 ALD cycles on the mesoporous film, the Hf XRF intensity increased much faster than during ALD on the planar substrate, proving that HfO_2 got deposited onto the interior surface of the ink-bottle mesopores (Figure 2b). As the deposition progressed, the slope of the Hf XRF intensity curve decreased and became more similar to the slope obtained for ALD on the planar substrate. This observation suggests that the pore necks became too narrow after 19 cycles of HfO_2 deposition and were no longer accessible for the Hf-precursor molecules (Figure 2c). From then on, ALD continued on top of the coated mesoporous film (Figure 2d).

In order to obtain more local and direct information of the mesoporous titania film coated with 30 ALD cycles of HfO_2, we applied transmission electron microscopy (TEM). Although this technique is often used in the study of porous materials, one should never forget that these images only provide a two-dimensional (2D) projection of a 3D object. In order to characterize the 3D structure, electron tomography is required.[19] In this technique, the specimen is tilted over an angular range, as large as possible, while acquisition of the same area of interest is made every 1 or 2 degrees. Next, the series of images is aligned and used as an input for a mathematical algorithm that reconstructs the 3D structure. In materials science, and also in this study, high angular annular dark field scanning (HAADF-STEM) is often the preferred technique to acquire the images of the tilt series because the intensity varies monotonically with composition and specimen thickness.[20] Since the intensity scales approximately to Z^2, HAADF-STEM allows for direct differentiation between the titania film and the HfO_2 ALD coating.

Figure 3a shows a 2D HAADF-STEM image of a focused ion beam prepared micropillar consisting of the Si substrate, the

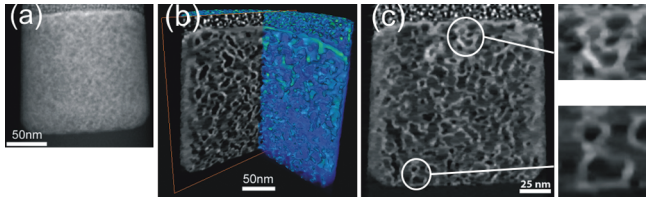

Figure 3. (a) 2D HAADF-STEM image of the micropillar sample, from top to bottom: Pt layer, mesoporous titania film coated with HfO_2, and Si substrate. (b) Slices through the 3D reconstruction. (c) *XZ*-orthoslice. Details showing conformally coated ink-bottle pores.

mesoporous titania thin film coated with HfO_2, and a Pt layer that was deposited for protection reasons. The 3D structure of the film could not be extracted from this single 2D image. The micropillar was mounted on an on-axis rotation tomography holder,[20,21] and a tilt series of this 2D type of images was recorded (more details can be found in the Supporting Information). The 3D structure of the sample was then reconstructed using a novel reconstruction algorithm for electron tomography called the total variation minimization (TVM) algorithm.[22] This algorithm is based on compressive sensing, a field in image processing specialized in finding a sparse solution or a solution with a sparse gradient to a set of ill-posed linear equations. The advantage is that the reconstruction is easier to segment and has a better signal-to-noise ratio. The 3D volume rendering of the mesoporous material coated with HfO_2 is shown in Figure 3b. To examine the inner structure in more detail, slices were made *through* the 3D reconstruction. Figure 3c shows such an *XZ*-orthoslice. A complete movie is shown in the Supporting Information. The light gray zones correspond to the HfO_2 coating, the dark gray zones to the titania pore walls, and the black zones to the voids. The details in Figure 3c show that the pores are ink-bottle shaped, but with cages that are far from spherical. From Figure 3c it is clear that the HfO_2 coating is uniformly deposited throughout the whole mesoporous film. The thickness of the HfO_2 coating on top of the mesoporous film was 3.4 ± 0.6 nm,

dx.doi.org/10.1021/cm203754a | *Chem. Mater.* 2012, 24, 1992–1994

whereas the thickness of the HfO_2 coating on the pore walls inside the film was only 2.2 ± 0.5 nm. This result confirms the interpretation of the in situ XRF data in Figure 2e: after ca. 19 ALD cycles the pore necks were no longer accessible for the Hf-precursor, and during the next 11 ALD cycles there was only deposition on top of the coated mesoporous thin film resulting in the higher HfO_2 thickness. The HfO_2 thickness that seems to clog the pore necks, 2.2 ± 0.5 nm, is in good agreement with the value expected based on the EP measurements. EP indicated an original neck size of ca. 4.8 nm, and thus a coating of ca. 2 nm is expected to shrink the neck size below the estimated diameter of the Hf-precursor molecule, ca. 0.7 nm. The electron tomography study also confirms that the cages were not completely filled with HfO_2, as expected based on the ink-bottle shape of the pores.

For most applications, it is, however, not the goal to create a porous film with inaccessible voids. Instead, for applications in catalysis and molecular separation, for example, it is of crucial importance that the mesopores are still accessible after ALD treatment. We utilized EP to quantify the accessible porosity after ALD of TiO_2 in the mesoporous titania film. Figure S2 in the Supporting Information shows the XRF data recorded in real time during 50 ALD cycles of TiO_2 in the ink-bottle mesopores. The Ti XRF intensity curve showed the same trends as the Hf XRF intensity curve plotted in Figure 2e. At ca. 40 ALD cycles the growth rate transitioned from a high value attributed to ALD inside the pores (Figure 2b,c) to a lower value indicating ALD on top of the coated pores (Figure 2d). Because the GPC of the TiO_2 process on a planar sample is roughly half the GPC of the HfO_2 process, it is not unexpected that 40 TiO_2 ALD cycles were needed to clog the pore necks as compared to the 19 HfO_2 ALD cycles. The toluene sorption isotherm measured after 50 TiO_2 ALD cycles is plotted in Figure 1a. It is clear that no toluene could be adsorbed in the pores, indicating that the pore necks are clogged due to the TiO_2 coating, confirming the interpretation of the XRF data.

According to the in situ XRF data, applying less than 40 ALD cycles would shrink the ink-bottle shaped mesopores without clogging their entrance. After 15 TiO_2 ALD cycles in the mesoporous titania thin film, the porosity decreased from ca. 27% to ca. 23% (Figure 1a), and the average pore and neck diameter were reduced to ca. 5.4 nm and ca. 3.6 nm, respectively (Figure1b,c). The sorption isotherm shows the same H2 type hysteresis loop as the isotherm measured on the original titania thin film, indicating that the original ink-bottle shape of the mesopores is retained after 15 cycles of TiO_2 ALD. After the deposition, the average pore and neck radii are quasi-equally reduced (by ca. 7 and 6 Å, respectively), proving the excellent conformality of the coating in the porous film.

In summary, we have characterized the ALD processes of TiO_2 and HfO_2 in ink-bottle shaped mesopores by a combination of in situ XRF, EP, and advanced electron tomography. Our results demonstrate that ALD is an excellent technique for tuning the pore size of ink-bottle shaped mesopores at the atomic level. Furthermore, our study proves that in situ XRF is an ideal approach to control the ALD process cycle-per-cycle. The methodology presented here is very attractive for the synthesis of novel molecular separation systems and catalyst supports.

■ ASSOCIATED CONTENT

Supporting Information

A movie of the 3D reconstruction (MPG) and experimental details (PDF). This material is available free of charge via the Internet at http://pubs.acs.org.

■ AUTHOR INFORMATION

Corresponding Author

*E-mail: jolien.dendooven@ugent.be.

Notes

The authors declare no competing financial interest.

■ ACKNOWLEDGMENTS

The authors acknowledge financial support from the ERC (Grant 239865), the Flemish Hercules 3 initiatives and DOE (Grant DE-FG02-03ER46037). J.D. and B.G. acknowledge the Flemish FWO for a Ph.D. grant. Use of the NSLS, BNL, was supported by DOE under contract no. DE-AC02-98CH10886.

■ REFERENCES

(1) Corma, A. *Chem. Rev.* **1997**, *97*, 2373.
(2) Schüth, F.; Schmidt, W. *Adv. Mater.* **2002**, *14*, 629.
(3) Trong, On, D.; Desplantier-Giscard, D.; Danumah, C.; Kaliaguine, S. *Appl. Catal., A* **2001**, *222*, 299.
(4) Detavernier, C.; Dendooven, J.; Pulinthanathu Sree, S.; Ludwig, K. F.; Martens, J. A. *Chem. Soc. Rev.* **2011**, *40*, 5242.
(5) Elam, J. W.; Routkevitch, D.; Mardilovich, P. P.; George, S. M. *Chem. Mater.* **2003**, *15*, 3507.
(6) Perez, I.; Robertson, E.; Banerjee, P.; Henn-Lecordier, L.; Son, S. J.; Lee, S. B.; Rubloff, G. W. *Small* **2008**, *4*, 1223.
(7) Pagán-Torres, Y. J.; Gallo, J. M. R.; Wang, D.; Pham, H. N.; Libera, J. A.; Marshall, C. L.; Elam, J. W.; Datye, A. K.; Dumesic, J. A. *ACS Catal.* **2011**, *1*, 1234.
(8) Muylaert, I.; Musschoot, J.; Leus, K.; Dendooven, J.; Detavernier, C.; Van Der Voort, P. *Eur. J. Inorg. Chem.* **2012**, 251.
(9) Libera, J. A.; Elam, J. W.; Pellin, M. J. *Thin Solid Films* **2008**, *516*, 6158.
(10) Kucheyev, S. O.; Biener, J.; Wang, Y. M.; Baumann, T. F.; Wu, K. J.; van Buuren, T.; Hamza, A. V.; Satcher, J. H., Jr.; Elam, J. W.; Pellin, M. J. *Appl. Phys. Lett.* **2005**, *86*, 083108.
(11) Sree, S. P.; Dendooven, J.; Korányi, T. I.; Vanbutsele, G.; Houthoofd, K.; Deduytsche, D.; Detavernier, C.; Martens, J. A. *Catal. Sci. Technol.* **2011**, *1*, 218.
(12) Dendooven, J.; Sree, S. P.; De Keyser, K.; Deduytsche, D.; Martens, J. A.; Ludwig, K. F.; Detavernier, C. *J. Phys. Chem. C* **2011**, *115*, 6605.
(13) Dendooven, J.; Devloo-Casier, K.; Levrau, E.; Van Hove, R.; Sree, S. P.; Baklanov, M. R.; Martens, J. A.; Detavernier, C. *Langmuir* **2012**, *28*, 3852.
(14) Pan, J. H.; Lee, W. I. *New J. Chem.* **2005**, *29*, 841.
(15) Baklanov, M. R.; Mogilnikov, K. P.; Yim, J.-H. *Mater. Res. Soc. Symp. Proc.* **2004**, *812*, F5.4.1.
(16) King, J. S.; Graugnard, E.; Summers, C. J. *Adv. Mater.* **2005**, *17*, 1010.
(17) Knez, M.; Kadri, A.; Wege, C.; Gösele, U.; Jeske, H.; Nielsch, K. *Nano Lett.* **2006**, *6*, 1172.
(18) Devloo-Casier, K.; Dendooven, J.; Ludwig, K. F.; Lekens, G.; D'Haen, J.; Detavernier, C. *Appl. Phys. Lett.* **2011**, *98*, 231905.
(19) Midgley, P. A.; Weyland, M. *Ultramicroscopy* **2003**, *96*, 413.
(20) Biermans, E.; Molina, L.; Batenburg, K. J.; Bals, S.; Van Tendeloo, G. *Nano Lett.* **2010**, *10*, 5014.
(21) Ke, X.; Bals, S.; Cott, D.; Hantschel, T.; Bender, H.; Van Tendeloo, G. *Microsc. Microanal.* **2009**, *16*, 210.
(22) Goris, B.; Van den Broek, W.; Batenburg, K. J.; Heidari Mezerji, H.; Bals, S. *Ultramicroscopy* **2012**, *113*, 120.